Oceanic loading monitored by ground-based tiltmeters at Cherbourg (France)

Nicolas Florsch, Muriel Llubes, Guy Wöppelmann, Laurent Longuevergne, Jean-Paul Boy

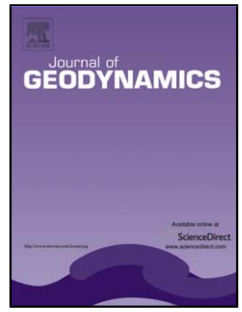

Title: Oceanic loading monitored by ground-based tiltmeters at Cherbourg (France)

Authors: Nicolas Florsch, Muriel Llubes, Guy Wöppelmann, Laurent Longuevergne, Jean-Paul Boy

PII: S0264-3707(09)00084-2
DOI: doi:10.1016/j.jog.2009.09.017
Reference: GEOD 911

To appear in: *Journal of Geodynamics*

Oceanic loading monitored by ground-based tiltmeters at Cherbourg (France)

Nicolas Florsch(*)[(1)], Muriel Llubes[(2)], Guy Wöppelmann[(3)], Laurent Longuevergne[(4)], Jean-Paul Boy[(5)]

(1) UMMISCO/IRD 32, avenue Henri Varagnat 93143 Bondy Cedex, France; UPMC, Paris, France; Dept of Mathematics and Applied Mathematics, UCT, South Africa.

(2) Université de Toulouse, OMP 14 av. Edouard Belin, 31400 Toulouse, France

(3) LIENSs/ULR, 2 rue Olympe de Gouges, 17000 La Rochelle , France

(4) Bureau of Economic Geology, Jackson School of Geosciences, The University of Texas at Austin, PO Box X, Austin, TX 78713, USA

(5) EOST/IPGS (UMR 7516 CNRS-ULP), 5 rue René Descartes, 67084 Strasbourg, France, and NASA GSFC, Planetary Geodynamics Laboratory, Code 698, Greenbelt, MD 20771, USA.

Abstract

We installed two orthogonal Blum-Esnoult silica tiltmeters in an underground military facility close to the shore in Cherbourg (France). They have recorded the ocean tide and the associated oceanic loading effects from March 2004 to July 2005. The signal to noise ratio is such that, within a period range from a few minutes to a few days, the main nonlinear oceanic tides up to the M10 group can be observed. The modelling of the tidal tilt deformation has been carried out using oceanic models of the FES2004 family, with a stepwise refinement of the grid size based on the unstructured grid T-UGAm model leading to the NEA-2004 tidal solution. This improvement permits to reduce the discrepancy between the model and the data with respect to the use of FES2004 alone, and show that, although the misfit remains significant, one progresses toward an independent mean to validate the oceanic models and finally the whole modelling process. We also show that tiltmeters open new opportunities to explore loading of non linear tides on a larger spectrum than gravimeters and GPS do.

Keywords

Inclinometry, tilt, oceanic loading, FES2004, nonlinear tides

1. Introduction

The oceanic loading phenomenon involves the attraction and deformation of the Earth that are due to the varying weight of moving water masses in the oceans and seas, mainly the oceanic tides. These effects may be measured on the ground by several geodetic observables: classically gravity, land level displacement, (Llubes *et al.*, 2001, Vey *et al.*, 2002, Llubes *et al.*, 2008), but also strain (Beavan, 1974) and more rarely stress (see for instance Willcok, 2001).

This paper is focused on the tilt effects generated by tidal oceanic loading on the French coast (Cherbourg, Cotentin region). The ocean tidal amplitude may reach there up to several meters.

While considering gravity variations in the vicinity of a sea with large tides, the proper loading contribution can reach about one third of the elastic earth tide variation (Llubes et al., 2001). Tilts are much more sensitive to the coastal loading since the lateral gradient of vertical displacement is involved measured rather than the amount of displacement, and the gradient reaches its maximum close to the coast. Actually the loading tilt itself reaches at Cherbourg about three times the solid tide tilt effect. Precisely, two factors converge to generate a large amplitude to the loading tilt locally: 1) the decreasing rate of the tilt Green function as a function of the load distance is more rapid with respect to gravity: the decreasing of the tilt Green function is close to and asymptotically as $1/r^2$ instead of $1/r$ in the gravity case (see for instance Farrell, 1972). This feature leads to a sort of homothetic invariance scale (Rerolle *et al.*, 2006) when integrating over an area which also depends on r^2; 2) Coastal areas are zones where the tidal amplitude is much greater than in the open ocean. Finally, these properties make the tiltmeters highly sensitive and suitable to study local loading phenomena.

Strictly speaking, tiltmeters record the variations of the gravity direction, more precisely the variations between the instantaneous geoid and the crust on which these instruments are settled. Both are affected by water loads. In practical terms, the only signal that can be measured is the difference between the geoid and the crust. It is not possible to refer tilts to a space or terrestrial reference frame because the accuracy that would be required to refer tilt data to this frame should be of the same order of magnitude than a tiltmeter resolution (at least), that is better than 10^{-9} rad at a few second time scale. Comparatively a one meter diameter zenithal telescope would have a 10^{-6} rad resolving power. Of course, it is only a practical limitation. Actually, the zero instrumental reference is just its initial state when beginning the record.

The geometrical and dynamical effects induced by the oceanic loads can be easily computed using the Green formalism (LLubes and Mazzega, 1997), which degenerates in a simple convolutive formalism as long as the Earth is considered as spherically symmetric. One specific Green function exists to describe the linear elastic Earth response to a local load in terms of, respectively, vertical and horizontal displacements, stress, strain and gravity. Green functions are available for different Earth models. We use here the functions devoted to tilts provided by Pagiatakis (1990) which are relative to a viscoelastic, rotating PREM-like Earth. (See also Boy *et al.* in this issue).

2. Experiment description and site corrections

2.1. Tiltmeters records

The tilmeters used in this experiment are very compact instruments historically designed by Blum (1962) (see also Saleh *et al.*, 1991) and nowadays built by Marie-France Esnoult at IPGP. These instruments are made with silica glass and are built according to Zöllner's pendulum concept. Tiltmeters require a two-step calibration: the first one is electronic (the sensitivity of the displacement probe) and the second one is purely mechanistic (the amplification of a pendulum is $1/\sin(\alpha)$, α being the angle between the rotation axe and the vertical line). Scientific and historical background of this kind of probes may be found in Melchior (1983). Braitenberg and Zadro (1999) also provide a suitable summary of their functioning.

The tiltmeters used in this experiment can reach a resolution of about 10^{-9} rad (Saleh *et al.*, 1991). Actually the gain accuracy (calibration constant) is expected to be better than 4 % at 1 σ. However, pendulums are affected by some "external" limitations. They are highly sensitive to very local environmental background variations: temperature, dampness of the floor where the instrument lies, and any kind of deformation of the stand. Generally speaking, a noticeable drift is observed on that kind of instruments, which is rarely understood in details. This drift could also involve the creeping of the tiltmeter components themselves: 10^{-9} rad variation over a 30 cm baseline is $0.3*10^{-9}$ m that is less than the elementary quartz crystal size. Hence, a suitable efficiency can only be reached thanks to exceptional settling conditions. In our experiment, two orthogonal pendulums have been installed in an unused part of a military underground facility owned by the French Marine, the "Souterrain du Roule", at Cherbourg (Figure 1). A drift does actually exist on both tiltmeters directions (EW and NS). However, it only causes interferences within the long period variations for more than one week, which can be eliminated by standard filtering methods to focus on the diurnal tidal band and its harmonics without spectral windowing artefacts.

2.2. Site effects

Site effects include topographic, cavity and geological effects. It is not only a magnification or reduction, new tilt signals can be added by strain-tilt coupling, typically resulting in a phase shift. The first who provided a useful approach to deal with such undesirable effects was Harrison (1976). An essential characteristic of site effects is the relative phase shift with respect to its theoretical value, which can reach as much as 40° (Lecolazet and Wittlinger, 1974).

In the paper by King *et al.* (1976) two issues dealing with the correction of site effects are mentioned: first the practical problem of constructing and checking large three-dimensional models, and second the difficulties of obtaining the correct input data for the models.

Nowadays, the Finite Element Method (FEM) could be applied (see for instance Kroner *et al.* 2005). These authors also remind the work of Itsueli *et al.* (1975) in which the problem of fractures or other inhomogeneities in the vicinity of the observation site, that cannot be adequately mapped (as in our case), are introduced. They proposed a method for removing the site effects without need for modelling by using a response method actually based on the seismic response of the Rayleigh waves. Neither of these methods can be used here. As stated by King *et al.* (1976) the first method is valid only for sites distant from ocean loading and the second requires at least the vertical component of the Rayleigh wave which is not available in our case.

However two points must be emphasized that show that site effects can be supposed to be small. Firstly, the crust flexure results mainly from remote surface loads and only involves Newtonian body forces as a minor contribution. The direct Newtonian attraction itself is tiny as it results from an elementary calculation. Indeed, the vertical deviation which is the main effect of the near oceanic attraction can be neglected, and then the associated cavity effect too. Secondly, tiltmeters have been installed more or less in the middle of the tunnel (a symmetry axis), where the disturbing effect is supposed to vanish.

The solution we finally adopted is neglecting potential site effect corrections, assuming it is less critical than in the frame of a body Earth Tide study. Finally, remembering that Lecolazet and Wittlinger (1974) attributed a significant phase shift to the cavity effect, we state that the undetectable phase difference between the observed and the modeled tidal tilt variations will be an *a posteriori* justification of the reduced rule of site effect.

2.3. Atmospheric contribution on tilt.

The atmosphere contributes to the tilt as any other moving mass (Boy *et al*, this issue). Two deformation processes have to be modeled: direct attraction (modifying the equipotential), and the elastic deformation due to the additional pressure on the crust, which also implies mass redistribution and thus an effect on the geoid (Farrell, 1972). The formalism to compute the atmospheric contribution is similar to that used in the oceanic or continental (hydrological) loading problems, except that one should consider here that the station is inside the atmosphere shell. As in the hydrological case, tilts are only influenced by the lateral pressure gradient (Rerolle et al., 2006). It implies that the classical admittance method cannot be applied in our case. Hence, two methods can be used to correct the atmospheric pressure contribution. First one could involve a local barometer network, which requires an extensive installation because of the different spatial scales involved in the deformation. Four barometers have been set up around the tilt site, 1 km from it. Unfortunately, this data did not attempt to provide accurate pressure effect prediction to correct the tilt time series. Some other experiences made recently in the Vosges Mountain, enforced by modeling computations, show that it would be necessary to have at our disposal both a tight network of barometer immediately around the tiltmeter and more remote ones to take into account atmospheric effects at severam spatial scales (Longuevergne, 2008). An aleternative method makes use of atmospheric data as provided by meteorological models. However, the sampling rate of these models is usually 6 hours, and does not allow to study phenomena below 12 hours. From a spectral point of view, pressure effects superimpose a rosy noise on periodic signals. If a good atmospheric pressure correction is expected to improve the S/N ratio, we suspect that it would be only a light improvement in our spectral analysis because the atmospheric enery is not concentrated on tidal peaks in the frequency domain. Precisely, let us consider the signal level close to M2. Figure 3 shows that is reaches about 0.003 μrad . Hence the pressure effect cannot exceed this level, wich is about 1/100 of the amplitude of M2. Then M2 is affected by less than 1% by the pressure effect. This is less than the calibration error, and then dropping the pressure effect will not cause serious misinterpretation. Similar reasonnings apply for the other harmonics. In addition, it is worth noticing that the pressure effect on that coastal border is complicated by the dynamic response of the ocean , refered as the “Inverted barometer hypothesis” (see Carrère and Lyard, 2003; Boy *et al.*, this issue). Finally, we dropped this correction which is practically difficult to perform, but in the same time probably not critical for our purpose, especially because the expected improvement will be obsolete when considering the poor calibration factor accuracy.

Traditional Earth Tide (ET) studies have benefited from gravity observations, such as the GGP experiment (http://www.eas.slu.edu/GGP/ggphome.html). Most of the geodesists consider that the discrepancies between tidal observations and corresponding models are very tiny. Actually, they are much smaller toward the inner continental stations where the influence of oceanic loadings is reduced. The agreement between the Love numbers used to compute visco-elastic Earth tides and those derived from GGP GGP (see Baker and Bos, 2003; Boy *et al.*, 2003) cryogenic gravimeter data is better than 1/100. This is indeed negligible when considering the tiltmeter factor calibration accuracy and one can assume that the modelled Earth tide elastic contribution is very accurate and can be subtracted from the raw data to keep only oceanic loading effects. Since cavity and site effect are assumed to be small, we consider that it is neither necessary to correct the Eart tide contribution for it to perform this substraction. Finally, we consider that the error associated with site effects is reduced due to (1) the position of the tiltmeters in the center of the tunnel and (2) the reduced amplitude of the Earth Tide by a factor 5 with respect to loading and (3) the feature of the tilt which involves limited body forces.

3. Signal processing and spectral analysis.

The whole time-series are available on request to the main author.

3.1 Basic spectral analysis

Tilts were initially sampled at 30 sec intervals. We applied high-pass filtering (to remove the drift) and resampling with low-pass filtering to avoid aliasing. This finally restricts the effective bandwidth to periods between 10 minutes and 72 hours. Raw and filtered signals are plotted in Figure 2. The amplitude spectra of the filtered signals are plotted on Figure 3. We chose a spectral normalization which preserves the amplitude of the periodic signal rather than the spectral power density. Hence, the tidal wave amplitudes can be directly read in microradians.

The spectra show several harmonics of the diurnal tidal waves. They are directly linked to the non-linear hydrodynamical waves in the English Channel and do not result from any kind of non-linearity of the Earth elastic response. Modelling the observed amplitudes requires the computation of these non linear waves by using the most complete oceanic charts, involving hydrodynamic modelling plus data assimilation, and to combine them with the rheological response of the Earth. However, the difficulties to retrieve upper order waves lie in the limitation in the mesh and restitution sharpness as seen by altimetric satellites; more exactly it depends on the trade-off between time and space sampling, both limited in practice (Cartwright and Ray, 1990). This becomes more difficult as the order increases, since the higher the order, the smaller the typical wavelength to be taken into account.

Several points should be highlighted here:

- the amplitudes of even orders are greater than for other harmonics. This is expected since they are successive harmonics of the M2 dominant group.
- Tiltmeters are able to record nonlinear waves up to 10 cycles/day. Note that neither loading gravity studies (Boy *et al*., 2004) nor any other integrative geodetic method have been able to “see” these higher harmonic signals (although they are clearly seen in tide gauge records, of course). Hence tiltmeters are confirmed to be very sensitive

tools to observe the deformation induced by oceanic tides at the regional scale, and can be used up to high harmonics to validate non linear oceanic models.

3.2. Tidal analysis

Earth tide analysis softwares are designed to estimate the transfer response of the Earth with respect to the astronomical gravity potential, usually providing the delta and gamma factors (Melchior, 1983). To search for higher tidal harmonics in the tiltmeter records, we therefore looked for tidal analysis tools which actually are standard within the sea-level community. We used the MAS software developed by Simon (2007) which implements a general method for analysing sea level heights. Pouvreau *et al.* (2006) compared MAS to the well-known and widely distributed T_TIDE software (Pawlowicz *et al.* 2002), and could not notice any significant difference from both sets of estimated tidal amplitudes at Brest. A drawback of the current T_TIDE release is, however, that it cannot analyse datasets longer than one-year, whereas MAS is successfully applied over periods even longer than a century.

Table 1 shows the main tidal constituents that we obtained from the ocean-like tidal harmonic analysis performed on the tiltmeter observations that were previously corrected for the Earth tides over the period 2004/03/09 to 2005/07/18. These analysis have been gathered here for comparion with the models discussed in the next paragraph, but those only involve the major eight constituents.

4. FES2004/NEA time modelling and testing increasing contributive distance

The modelling is performed by combining FES2004 global oceanic model (Lyard *et al*. 2006), and the refined NEA (North East Atlantic tidal solution) model in the close Atlantic and English Channel (Pairaud *et al.*, 2008). To perform the computation, the jointed model heights are convolved in two dimensions by using the radial tilt Green Function provided in Pagiatakis (1990).

We have plotted on Figure 4 the modelled oceanic loading and the Earth Tide contribution, as well as the sum of these two signals and compared them with the observation. The chosen window permits to illustrate the best and the worst agreements. The largest discrepancies between modelled and observed oceanic loading occur for large tidal ranges. At the end of the window, during small tidal ranges, the agreement is far better. In general, the EW component is better modelled than the NS component. This may be linked to the orientation of the coast (EW) which is located 2 km northwards of the observing site.

We do not know the origin of these discrepancies and their variations in time. However, we form the hypothesis that it could come from the interference arrangement between the main tidal M2 group and the overtones (nonlinear harmonics). We only took into account 8 waves in the diurnal and semi-diurnal bands here and none of the non-linear tides.

Sensitivity of the tilts to the remoteness of the loads.

To study the tilt as a function of the distance to the loads, we chose an adapted geographical windowing, as shown in Boy *et al.* (2003) to represent the different contribution of individual areas.

The computation was performed by distinguishing three exclusive zones: this enabled to study the influence of nearby, medium range and remote oceanic loading effects. Zone 1 (Z1): from -5° to 1.5° in longitude and 48.5° to 51.25° in latitude, based on NEA2004 model (Pairaud *et* *al.*, 2008) corresponds to the English Chanel; Zone 2 (Z2): from -20° to 14° in longitude and 30° to 61° in latitude, also based on NEA2004 model, is a medium range zone excluding Z1. Zone 3 (Z3), based on FES2004 (Lyard *et al.*, 2006), is global and covers the other parts of the world excluding Z1 and Z2.

Figure 5 shows the M2 wave amplitude and the three zone boundaries. Figure 6 highlights the cumulative contributions of each of these 3 zones for all the diurnal and semi-diurnal waves. It clearly showed the effect of the local magnification in the semi-diurnal band (N2, M2, S2, and K2). Large zooms were required to see further contributions; the local contribution was definitely dominant, and one could neglect the farther load contributions in the model without significant loss.

The diurnal waves (O1, P1, K1, Q1) formed a second class of patterns. Though the local zone (English Channel) dominated the signals, the Atlantic and remote zones were almost of the same order of magnitude and none of the contributions could be neglected. This could be explained by the fact that the diurnal waves were not as amplified by the Channel as the semi-diurnal waves.

5. Comparison between final model and observed data.

The phasor diagram given in Figure 7 shows the residual discrepancy between the observed data (from which the Earth Tide contribution was previously removed) and the models. Using FES2004 alone provided results that were not in good agreement with the observations, especially as far as the NS component is concerned. By substituting FES2004 with NEA2004 in the area close to the site, a real improvement is achieved, but a significant discrepancy remains. Since the main improvement arising from FES2004 to NEA is the finer spatial resolution of the grid used in the computation, one could conclude that the residual discrepancy was mainly due to the coarseness of the grid still in use, which is a more critical issue when dealing with tilt than when dealing with gravity or vertical displacement time-variations. The successive points "FES2004", "FES2004+NEA" are often quite on a line that seems on the way to tend to the observation: see M2, S2, K2, K1. The improvement appeared to be better on the NS component than on the EW one.

The less the amplitude of the wave, the less the relative accuracy of this line pattern; see for instance the EW component of Q1. In such case, it is likely that the random noise still hide the signal and/or prevent the model to be accurate.

6. Discussion and Conclusions

The sensitivity of the tiltmeters allows to observe the loading effect with a high signal/noise ratio. This implies that assuming a known mechanical response of the Earth, tiltmeters can be used to validate oceanographic models and nonlinear tides. Contrary to tide gauges whose spatial sensitivity is strictly local (and can be affected by the harbour inner architecture), the tilt offers an integrative measurement of the behaviour of the ocean with a regional spatial sensitivity. This is the case for the M2 group; the wave amplitude is quickly decreasing when the distance to the coast increases, making the remote contribution really negligible. The main remaining issues are: 1) the site effect, which is difficult to estimate in most cases, 2) the lack of atmospheric detailed data to correct for pressure within this short period band, and 3) the necessity to take into account a dynamical and coupled atmosphere-ocean modelling (see Boy *et al.*, this issue), 4) the difficulty to achieve a good accuracy in the calibration factor for this kind of tiltmeters. Further improvement of the computing grid sharpness will certainly improve the fit and all these challenges could be tackled in the future. Currently new experiments are carried on in Brittany near Ploemeur in France (Bour *et al.*, 2008) which could serve to improve our knowledge. Indeed, long-base hydrostatic tiltmeters have been set up in shallow galleries. They have been recording for a few months. Both calibration uncertainties and site effects will be easier to solve there for that kind of instruments. In parallel, atmospheric sampling rates and coupled modelling with the oceans are continuously improving.

Due to its features and assuming further improvements, tilt could become a systematic tool to test oceanic models as far as non linear high harmonics are concerned. Neither gravity nor GPS techniques are able to see M4, M6, M8 and M10 waves with such a signal/noise ratio as the one reached by tiltmeters today.

Acknowledgement

We thank Marie-France Esnoult and Karim Mahiouz for installing the tiltmeters, Jacques Delorme and the French Marine for providing the Roule gallery to install the tilt-meters. We would also like to thank Bernard Simon (SHOM) for kindly providing us his tools (MAS) in order to apply the ocean tidal-like analyses to the tiltmeter records. This study has been supported by the program CNRS-DBT and the grant in the frame of the multi-organisation GDR-G2. Nicolas Florsch is currently welcomed at the Department of Mathematics and Applied Mathematics at Cape Town University, South Africa, and is granted by the French Organization "Institut de Recherche pour le Développement". Jean-Paul Boy is currently visiting NASA Goddard Space Flight Center, with a Marie Curie International Outgoing Fellowship (N° PIOF-GA-2008-221753).

We thanks the anonymous reviewer who made very constructive review. We thank H.-G. Scherneck and a anonymous referee for their comments and suggestions that helped in improving the manuscript.

References

Baker, T.F. and M. S. Bos, 2003. Validating Earth and ocean tide models using tidal gravity measurements. Geophys. J. Int., 152, 468-485.

Beavan, R.J., 1974. Some Calculations of Ocean Loading Strain Tides in Great Britain, Geophys. .J. R. Astr. Soc. ,Vol . 38, 1, pp. 63-82.

Blum, P., 1962. Contribution à l'étude des variations de la verticale en un lieu, Ann. Geophys., 19, 215–243.

Bour, O., Caudal, J.P., Le Borgne, T., Moreau, F., Labasque, T., Boudin, F., Aquilina, L., Ruelleu, S., Dauteuil, O., Jacob, T., Durand, S., Maia, M., Biessy, G., Tarits, C., Bayer, R., Le Moigne, N., Morel, L., Henin, O., Ferrand, A., Davy, P., 2008. The Ploemeur research site : goals and motivations for long-term monitoring and groundwater experiments, AGU Fall Meeting, San Francisco, USA, 15-19 December 2008.

Boy, J.P., Llubes, M., Hinderer, J., and Florsch, N., 2003. A comparison of tidal ocean loading models using superconducting gravimeter data. J. Geophys. Res., 108, B4, 2193, doi: 10.1029/ 2002JB002050, 2003.

Boy, J.-P., M. Llubes, R. Ray, J. Hinderer, N. Florsch, S. Rosat, F. Lyard and T. Letellier, 2004, Non-linear oceanic tides observed by superconducting gravimeters in Europe, J. Geodyn., 38, 391-405.

Boy, J.-P., L. Longuevergne, F. Boudin, T. Jacob, F. Lyard, M. Llubes, N. Florsch and M.-F. Esnoult, 2009. Modelling atmospheric and induced non-tidal oceanic loading contributions to surface gravity and tilt measurements, J. Geodyn., this issue.

Braitenberg.C., and Zadro, M., 1999. The Grotta Gigante horizontal pendulums - instrumentation and observations. Bollettino di Geofisica Teorica ed Applicata, 40 , no 3-4, pp. 577-582.

Carrère, C. and F. Lyard, 2003. Modeling the barotropic response of the global ocean to atmospheric wind and pressure forcing - Comparisons with observations, Geophys. Res. Lett., 30 (6), 1275, doi:10.1029/2002GL016473.

Cartwright, D.E., and Ray, R.D., 1990. Oceanic tides from Geosat altimetry. J. Geophys. Res., 95 (C3), pp. 3069–3090.

Farrell, W., 1972. Deformation of the Earth by surface load, Review of Geophysics Space Physics, 10(3), 761–797.

Harrison, J. C., 1976. Cavity and topographic effects in tilt and strain measurements. J. Geophys. Res., 81, 319 – 328

Itsueli, U.J., Bilham, R.G., Goulty, N.R., and King, G.C.P., 1975. Tidal strain enhancement observed across a tunnel, *Geophys. J. R. astr.Soc*., **42**, 555

King, G., Zürn, W., Evans, R., Emter, D., 1976. Site Correction for Long Period Seismometers, Tiltmeters and Strainmeters. Geophysical Journal International, vol. 44, issue 2, pp. 405-411.

Kroner, C., Jahr, T., Kuhlmann, S., & Fisher, K., 2005. Pressure-induced noise on horizontal seismometer strainmeter records evaluated by finite element modelling, Geophys. J. Int., 161, 167–178.

Lecolazet, R. & Wittlinger, G., 1974. Sur l'influence perturbatrice de la deformation des cavités d'observation sur les marées clinométriques, C. R. Acad. Sc. Paris, 278, 663–666.

Llubes, M., and Mazzega, P., 1997. Testing recent global ocean tide models with loading gravimetric data, Progress In Oceanography, 40, 1-4, pp. 369-383, doi:10.1016/S0079-6611(98)00014-7

Llubes, M., Florsch, N., , Amalvict, , M., Hinderer, J., Lalancette, M.F., Orseau, D., et Simon, B., 2001. Observation gravimétrique des surcharges océaniques : premières expériences en Bretagne. C.R. Acad. Sci, Earth and Planetary Sciences 332, 77-82.

Llubes, M., Florsch, N., Boy, J.P., Amalvict, M., Bonnefond, P., Bouin, M.N., Durand, S., Esnoult, M.F., Exertier, P., Hinderer, J., Lalancette, M.F., Masson, F., Morel, L., Nicolas, J., Vergnolles, M., Wöppelmann, G., 2008. Multi-technique monitoring of ocean tide loading in Northern France. C. R. Geoscience 340, 379–389

Longuevergne, L. (2008), Contribution a l'Hydrogéodésie, Ph.D. thesis, 300 pp, Université Pierre et Marie Curie. Can be downloaded at :
http://tel.archives-ouvertes.fr/index.php?halsid=0tl01nopdml7t5508qotbnu7v1&view_this_doc=tel-00319205&version=1

Lyard, F., Lefevre, F., Letellier, T., and Fracis, O., 2006. Modelling the global ocean tides: modern insights from FES2004. Ocean Dynamics, 56, 5-6, 394-415. DOI 10.1007/s10236-006-0086-x.

Melchior, P., 1983. The Tides of the Planet Earth, Pergamon Press.

Pagiatakis, S., 1990. The response of a realistic Earth to ocean tide loading, Geophys. J. Int., 103, 541–560. DOI: 10.1111/j.1365-246X.1990.tb01790.x

Pawlowicz, R., Beardsley, B., and Lentz, S., 2002. Classical tidal harmonic analysis error estimates in MATLAB using T_TIDE. Comput. Geosci. 28, 929–937.

Pairaud, I.L., Lyard, F., Auclair, F., Letellier, T., Marsaleix, P., 2008. Dynamics of the semi-diurnal and quarter-diurnal internal tides in the Bay of Biscay. Part 1: Barotropic tides. Continental Shelf Research 28 (2008) 1294– 1315.

Pouvreau, N., Martin Miguez, B., Simon, B, and Woppelmann, G., 2006. Evolution of the tidal semi-diurnal constituent M2 at Brest from 1846 to 2005. C. R. Geoscience, 338, pp. 802–808.

Rerolle, T. , Florsch, N., Llubes, M., Boudin, F., and Longueverg,e, L., Inclinometry, a new tool for the monitoring of aquifers? C. R. Geoscience 338 (2006). doi:10.1016/j.crte.2006.07.004

Saleh, B., Blum, P.A., and Delorme, H., 1991. New silica compact tiltmeter for deformations measurements, J. Survey Eng. 117 , pp. 27–35.

Simon, B, 2007. La marée oceanique côtière. Collection “Synthèses”, Ed. Insitut Océanographique, 433 pp.

Vey,S. , Calais, E., , Llubes, M., Florsch, N., Woppelmann, G., Hinderer, J., Amalvict, M., Lalancette, M.F., Simon, B., Duquenn F., Haase, F.S., 2002 GPS measurements of ocean loading and its impact on zenith tropospheric delay estimates: a case study in Brittany, France. Journal of Geodesy, vol. 76, 8, pp 419-427.

Wilcok, W.S.D, 2001. Tidal triggering of microearthquakes on the Juan de Fuca Ridge. GRL, Vol. 28, N° 20, pp. 3999-4002,.

Table captions

Table 1 shows 1) the main tidal constituents obtained from the ocean-like tidal harmonic analysis performed on the tiltmeter observations that were previously corrected for the Earth tides over the period 2004/03/09 to 2005/07/18; 2) the prediction of amplitude and phase for 8 waves based on FES2004 and NEA2004 model

Figure captions:

Figure1 : Site location and installation of a Blum Pendulum in the "Souterrain du Roule" at Cherbourg (France)

Figure2 : EW and NS raw and band-pass filtered tilt records at Cherbourg

Figure 3 : Fourier analysis (periodogramms) of the tilt records reveal a high signal/noise ratio of 100 (40 dB) at 2 cycle/day. Peaks are visible even at 10 cycles/day.

.

Figure 4: on the bottom part, Earth tide and loading models are shown separately, while there are summed in the top part of the figure. In both cases, the observation is also plotted and shows a greater amplitude than the model. The misfit could be due to non-linear tides that are not included in this computation.

Figure5 : M2 amplitude from FES2004 model (top), and NEA-2004 (bottom). The NEAmodel is computed by using an unstructured grid called T-UGAm (Courtesy I.L. Pairaud et al., 2008). The figure also shows the three zones used to perform the computation with increasing involved radius and surface, Zones 1, 2 and 3 as described in the text.

Figure 6: phasor diagram of the cumulative contribution of the 3 different zones for all diurnal and semi-diurnal waves.

Figure 7: phasor diagram showing the observation and how the model FES2004 and FES2004 improved with NEA tend to fit the data.

Table 1

Component		NS						EW					
Tidal constituent		Observation		FES+NEA 2004		FES 2004		Observation		FES+NEA 2004		FES2004	
Name	Doodson	Amp (nrad)	Phase (°)	Amp (nrad)	Phase (°)	Amp (nrad)	Phase (°)	Amp (nrad)	Phase (°)	Amp (nrad)	Phase (°)	Amp (nrad)	Phase (°)
M2	BZZZZZZ	394.22	250.9	265.19	257.1	196.79	264.7	437.19	326.3	367.37	333.7	335.06	334.8
S2	BBXZZZZ	137.88	291.0	89.33	298.0	69.04	300.1	149.13	8.3	128.5	21.5	111.11	4.5
N2	BYZAZZZ	82.45	232.5	45.76	236.0	40.00	264.7	86.92	308.9	70.48	317.4	63.26	315.6
K2	BBZZZZZ	40.14	287.9	23.40	293.3	16.01	299.8	40.31	1.1	28.51	27.2	28.63	19.8
K1	AAZZZZA	25.25	147.2	13.87	136.6	9.85	136.3	33.25	275.5	9.45	279.1	8.02	275.5
O1	AYZZZZY	5.00	63.8	9.78	28.1	6.05	26.9	18.03	242.6	7.99	160.1	7.23	159.4
P1	AAXZZZY	9.21	127.9	5.14	135.6	3.26	300.1	12.17	294.2	3.17	276.5	2.82	274.7
Q1	AXZAZZY	4.51	300.8	2.83	344.8	3.24	360.0	2.21	267.9	2.85	112.9	2.46	112.5
M4	DZZZZZZ	3.04	8.4					1.22	84.6				
MS4	DBXZZZZ	1.88	68.0					0.84	138.6				
MN4	DYZAZZZ	1.03	344.6					0.46	68.5				
M6	FZZZZZZ	0.65	90.4					0.37	268.8				
2MS6	FBXZZZZ	0.77	137.9					0.31	317.1				
2MN6	FYZAZZZ	0.46	65.4					0.17	230.5				
5MS8	HXBZZZZ	0.76	60.9					0.15	5.7				